Article

# Thermodynamic Performance Analysis of High Thermal Conductivity Materials in Borehole Heat Exchangers in the European Climate

Sanober Khattak, Borja Badenes, Javier Urchueguia and Burkhard Sanner

# Thermodynamic Performance Analysis of High Thermal Conductivity Materials in Borehole Heat Exchangers in the European Climate

Sanober Khattak [1,*], Borja Badenes [2], Javier Urchueguia [2] and Burkhard Sanner [3]

1 School of Engineering and Sustainable Development, Faculty of Computing, Engineering and Media, De Montfort University, Leicester LE1 9BH, UK
2 Information and Communication Technologies versus Climate Change (ICTvsCC), Institute of Information and Communication Technologies (ITACA), Universitat Politècnica de València, Camino de Vera S/N, 46022 Valencia, Spain
3 UBeG GbR, 35580 Wetzlar, Germany
* Correspondence: sanober.khattak@dmu.ac.uk

**Abstract:** While heat pumps have been acknowledged as a key enabling technology to achieve Net Zero goals, their uptake is limited by their performance and cost. In this paper, a simulation-based study is conducted to analyse the performance of ground source heat pumps (GSHPs) utilising high thermal conductivity materials for the borehole heat exchanger (BHE) pipe (1 W/mK) and grouting (3 W/mK) developed in the GEOCOND project. Exergy analysis is conducted to account for energy quantity and quality with a focus on BHE performance. An annual hourly simulation was performed using DesignBuilder V5.4 and Earth Energy Designer (EED4) for representative cool and hot locations in Europe—Stockholm and Valencia, respectively. For a constant BHE length, the results for Stockholm show that the high conductivity materials result in an increase of about 13% BHE exergy extraction compared to the standard grout and pipe, but no such improvement was observed for Valencia. The difference between outdoor temperature and its dynamic variation from the indoor setpoint is identified as a key factor in the overall GSHP exergetic performance. In future research, we propose a thorough life cycle analysis across diverse locations and varying indoor comfort criteria to pinpoint areas where the high thermal conductivity material can enable cost-effective, sustainable heating and cooling.

**Keywords:** ground source heat pumps; exergy analysis; low carbon heating; Net Zero; buildings energy modelling

## 1. Introduction

Heat pumps are a mature technology that can be coupled with renewable energy to deliver low carbon heating and cooling. Thus, they have been identified as a key enabling technology to decarbonise buildings space conditioning towards achieving Net Zero goals [1]. Typical heat pump installations are air source heat pumps (ASHPs) that suffer from relatively lower efficiencies owing to weather fluctuations and low winter air temperatures. Ground source heat pumps (GSHPs) are comparatively more energy efficient, as they take advantage of fairly stable underground temperatures, but the relatively higher cost over their lifecycles is a key barrier for their uptake.

The complete life cycle of the GSHP includes production, manufacturing, the use phase, and finally end-of-life disposal [2]. The dominant phase within this life cycle of a heat pump in terms of energy use and environmental impact is the "use phase" [2,3]. This is because heat pumps have a long useful life (>20 years) during which the heating and cooling energy demand may be delivered to the building continuously. In the use phase, the environmental impact and cost is dependent on the GSHPs' thermodynamic

performance, as greater efficiency translates to delivering the required heating or cooling with less electricity input and a lower cost and carbon footprint.

Grout thermal conductivity is widely recognized as a crucial parameter for the performance of ground source heat pump (GSHP) systems. This observation is evidenced by numerous studies, with Dong et al. [4] highlighting the need for in-depth theoretical investigation of material properties that impact thermal conductivity, including the dual influence of water-to-cement and sand-to-cement ratios. Badenes et al. [5] conducted a numerical study to identify target physical properties of grout and piping for enhanced GSHP performance. They showed that enhanced thermal conductivity has a positive impact on system performance. Similarly, Zhou et al. [6] developed a numerical model to probe the effect of grout thermal conductivity on heat transfer performance in borehole heat exchangers. Frac et al. [7] further developed grouts with a novel binder characterized by high thermal conductivity specifically designed for low-temperature geothermal applications.

Despite this focus on grout thermal conductivity and GSHP performance, most of the existing studies—including those by Dong et al. [8], Huang et al. [9], and Zhou et al. [6] —present analysis workflows that treat the GSHP system as an isolated unit separate from the building energy demand it is intended to service. This creates a discrepancy, as GSHP systems are essentially integrated systems designed to meet the heating and cooling demands of buildings.

The studies by Mahon et al. [10], Zhou et al. [6], and Deng et al. [11] explore GSHP systems from various angles such as seasonal thermal energy storage, techno-economic optimization, and ventilation rate influences on GSHP efficiency. Nevertheless, they do not integrate these analyses with building energy modelling (BEM), which is critical for a holistic understanding of GSHP performance in real-world applications. Furthermore, while some investigations such as those by Habibi et al. [12] and Tang and Nowamooz [13] have carried out energy and exergy analysis of heat pump systems and borehole heat exchangers respectively for a more rigorous thermodynamic treatment, there is limited evidence of such analysis in the context of grout thermal conductivity, especially analysis that incorporates BEM.

In essence, there is a clear need for research that integrates GSHP performance analysis with BEM, and simultaneously incorporates an exergy analysis for a rigorous thermodynamic evaluation. Such research would provide a comprehensive understanding of GSHP system performance, taking into account its interaction with the serviced building under varying weather conditions and considering the quality and quantity of energy involved.

To address this knowledge gap, in this paper, a simulation-based study is conducted to analyse the performance of ground source heat pumps (GSHPs), utilising high thermal conductivity materials for the borehole heat exchanger (BHE) pipe and grouting developed in the GEOCOND project [5]. This process is performed for the two representative hottest and coolest locations in Europe, Stockholm and Valencia.

## 2. Exergy Analysis for Thermodynamic Performance Analysis of GSHPs

When energy is delivered to buildings, it undergoes various transformations depending on the technology used. For the case of heat pumps, electrical energy is supplied and transformed to low-grade thermal energy, fulfilling a building's heating and cooling demand. While the quantity of energy remains conserved through the various transformations, its quality is degraded due to the loss of useful work that can be extracted from it. Indeed, a similar quantity of electricity is more useful as compared to low-grade thermal energy [14–16]. Unfortunately, this loss of energy quality is not considered in energy analysis. However, exergy, a thermodynamic property of the system and surroundings, accounts for both energy quantity and quality. Thus, it has been amply used for buildings thermodynamic performance analysis, including energy systems such as GSHPs [17–21].

Exergy is defined as "The maximum theoretical useful work (shaft work or electrical work) obtainable as the system is brought into complete thermodynamic equilibrium with the thermodynamic environment while the system interacts with this environment

only" [22,23]. It represents the variation of a mass or energy flow from the equilibrium state, which is effectively a representation of its useful work potential, and is measured in the same units as energy is. While exergy can be calculated for any mass or energy flow [24], for the case of buildings it is typically electricity and heat flows. As electricity is, by definition, pure work, its energy and exergy content are the same (Equation (1)).

$$\Delta E_{elec} = \Delta Ex_{elec} \tag{1}$$

For heat flows, the exergy content depends on the quantity of thermal energy ($Q$), the outdoor dry-bulb temperature ($T_0$), and the temperature of the heat flow as it crosses the system boundary ($T$) (Equation (2)).

$$Ex_{heat\ flow} = Q\left(1 - \frac{T_0}{T}\right) \tag{2}$$

The "LowEx" approach was developed to improve the exergetic performance of buildings, which aims to match the quality of energy supply and demand, thus minimising thermodynamic losses [25–27]. Equation (3) provides the exergy balance equation in which the exergy lost due to loss of energy quality is termed as exergy destruction [23]. In the equation, $Ex_{in}$ is the exergy entering the system, $Ex_{out}$ is the exergy leaving system, $\Delta Ex$ is the exergy change, while $Ex_{dest}$ is the exergy destruction due to thermodynamic irreversibilities (such as loss of energy quality).

$$Ex_{in} = \Delta Ex + Ex_{out} + Ex_{dest} \tag{3}$$

In Figure 1, the illustration depicts different energy sources and their respective applications within buildings, accompanied by an indication of energy quality. For instance, the utilization of high-quality energy sources such as oil for low-quality energy demands like space heating results in a significant reduction in energy quality. Alternatively, the utilization of ground heat for the same purpose mitigates the loss of energy quality and reduces exergy destruction, thus improving the matching of energy quality between the supply and demand in the building.



**Figure 1.** Examples of variation in energy quality in supply and demand for buildings [28].

While ground source heat pumps (GSHPs) require electricity, they also harness the heat from the ground, aligning energy quality more effectively with the demands of space heating and cooling. In a comparative study by Lohani and Schmidt [29], which evaluated ground and air source heat pumps and a conventional boiler in a typical residential setting, GSHPs emerged as the most energy and exergy efficient technology. The importance of borehole heat exchanger (BHE) performance in GSHP systems is underscored, as it directly influences the extraction of low-grade thermal energy from the ground.

Kizilkan and Dincer [16] delved into the thermodynamic performance of a borehole thermal energy storage system integrated with a GSHP, focusing on a university building in Ontario, Canada. Their findings indicated an overall exergy efficiency of 42.35%, with significant exergy loss attributed to declining energy quality. Similarly, Hu et al. [30] conducted an exergy analysis of a GSHP system for a Canadian public building, enhancing its exergy efficiency from 9% to 10.4% through an improved heat pump control strategy. Verda et al. [31] examined the design of a horizontal shallow GSHP system, revealing a 60% increase in BHE-extracted exergy when the ground loop depth was elevated from 1m to 2 m. Shifting focus to industrial contexts, Erbay et al. [32] scrutinized a GSHP utilized for food drying, achieving a remarkable exergy efficiency of 77%. This result stemmed from effective energy quality matching between supply and demand, particularly notable given the high heat requirement (70 °C) and cool ambient temperatures (10 °C) in the region. Ally et al. [33] analysed a vertical BHE application for residential space conditioning, showcasing that over 75% of the necessary energy was extracted from the ground. However, exergy efficiency for the GSHP was not computed. It is worth noting that due to the inherently low energy quality of space conditioning, the converted exergy value of the extracted energy could be significantly smaller.

Turning to building cooling, Menberg et al. [34] conducted an exergy analysis of a hybrid GSHP system, revealing higher efficiencies for heating (30%) compared to cooling (15%). Similarly, Kayaci, N. [35] pursued the design of a GSHP for an office building in Istanbul, utilizing exergetic and economic analyses. They deduced exergy efficiencies ranging from 36% to 39% over a decade of dynamic simulation data.

This brief review indicates the use and importance of exergetically analysing GSHP systems. The performance metrics (i) BHE exergy extraction and (ii) exergy efficiency have been used to assess thermodynamic performance. The exergy efficiency of the GSHP in the reviewed studies has ranged from 9–42% for building space conditioning applications. This low exergy efficiency is an indicator of the need to minimize electrical energy supply, which could be done by maximizing the BHE exergy extraction. Therefore, this paper aims to quantify the improvement achievable in a typical vertical U-tube BHE through the use of novel grouting and pipe materials developed in the GEOCOND project to provide valuable information in the use phase of the GSHP life cycle.

## 3. Methodology

### 3.1. Scope of Work and Simulation Approach

The scope of this study is limited to the use phase of the GSHP lifecycle, analysed using annual dynamic simulations (Figure 2). The analysis is conducted based on hourly data that includes (i) the weather conditions (hourly weather data from [36]), (ii) BHE design (iii), and building characteristics. The need to consider hourly variations in exergy analysis arises from the fact that exergy is also a function of the environment, and exergetic results are sensitive to the reference environment temperature. In addition, for the ground thermal response, the 10th simulated year was used to ensure that steady conditions in the BHE are reached. The system boundary for the heat pump system corresponds to "seasonal performance factor $H_1$ ($SPFH_1$)" [37], which includes the heat pump only and is well suited for analysis in the use phase. Consequently, the performance of the system is assessed in terms of (i) the exergy extracted from the BHE as an indicator of the BHE performance and (ii) the exergy efficiency of the house heating/cooling system.

The energy demand of a typical European residential house was generated using DesignBuilder V5.4 [38]. Using the hourly demand profile, the BHE was sized using the software EED 4.20 [39], while the exergy analysis was completed in MS Excel. The Earth Energy Designer (EED) software is a standard tool for designing energy systems using borehole heat exchangers (BHE) and has been extensively used in European projects. The EED 4 as used in this study offers hourly resolution for heating/cooling loads and output. While validated against full numerical simulation tools, EED's speed advantage over numerical simulations enables handling the high case and iteration demands of

GEOCOND exergy analysis (Bohne et al. [40] and Sanner et al. [41]). Moreover, the results generated in this study are taken from the simulated 10th year of operation, so that stable ground conditions are reached, and the initial transient effects of ground heating or cooling do not impact the analysis.
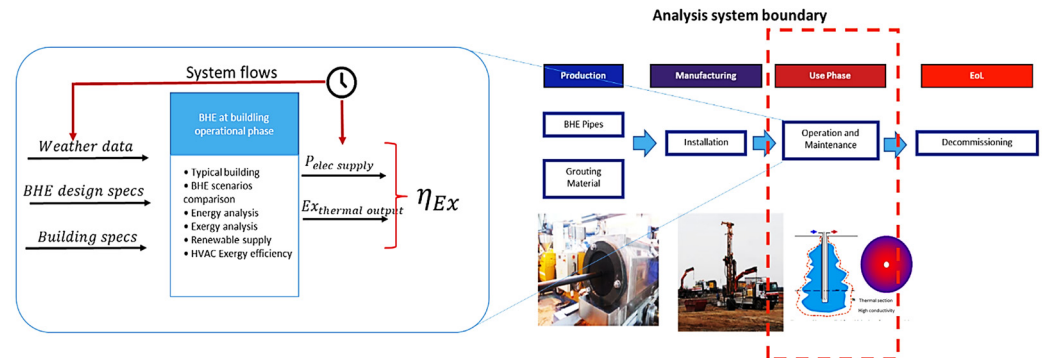


**Figure 2.** Analysis system boundary with a focus on the use phase.

Figure 3 depicts the simulation workflow, along with the data inputs/outputs at each step of the process. Initially, a fixed typical heat pump coefficient of performance (COP) was taken. This was varied iteratively until there was no change in the heat pump COP and the energy supplied by the GSHP which matched the demand profile of the building.
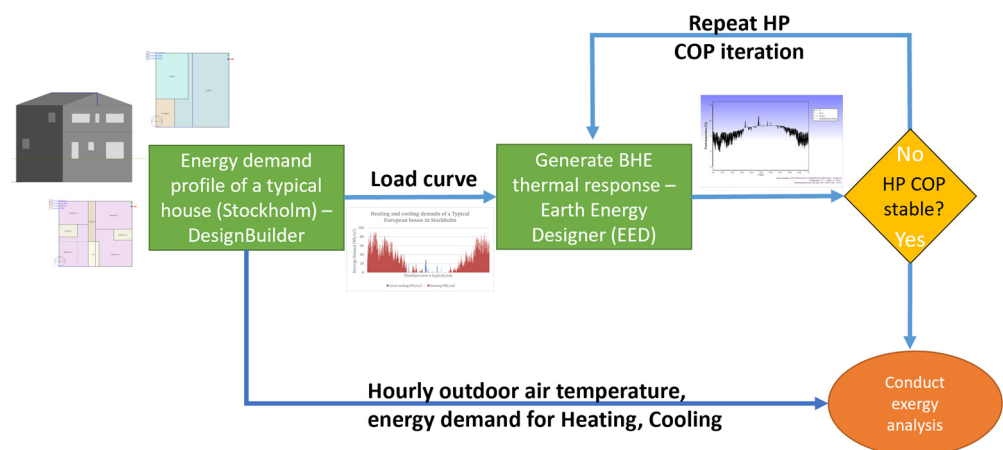


**Figure 3.** Simulation approach workflow.

### 3.2. Scenarios Definition

Keeping the building, location, and heat pump the same, performance comparison between the conventional BHE design and GEOCOND interventions was conducted. For the heat pump, a typical market available technology has been chosen in this study, specifically the Ochsner 10–12 kW dual heating and cooling mode heat pump [42]. Two locations, representative of cool and warm climates in Europe, were considered, namely Stockholm and Valencia, respectively. The considered building is a typical house, detailed in Section 3.3. A typical U-tube BHE was considered (about 100 m depth [43]). Corresponding to the building energy demand, BHE sizing in EED4 resulted in BHE lengths $2 \times 107$ m and $1 \times 190$ m for Stockholm and $2 \times 100$ m for Valencia. The two variations for Stockholm were considered to analyse the effect of increased BHE depth. Table 1 provides the details for the BHE characteristics used in the baseline scenario for Stockholm. For each location/BHE length, the following GEOCOND interventions were defined:

1. Baseline: This reference scenario is representative of the material and performance achievable using state of the art materials for BHE construction. Specifically, this includes the BHE pipe and grout. Badenes et al. [5] document the developments in pipe and grouting material achieved in the GEOCOND project. The baseline

corresponds to the PE100 pipe (thermal conductivity of 0.42 W/mK) and a grout with thermal conductivity of 2 W/mK.

2. Semi-GOECOND: The pipe used is the standard PE100 but with the improved GEO-COND grout (thermal conductivity of 3 W/mK).

3. GEOCOND: In this scenario, both the pipe and grouting used GEOCOND materials, with thermal conductivity values of 1 W/mK and 3 W/mK, respectively.

**Table 1.** BHE characteristics for Stockholm 2 × 107 m in the baseline scenario. For the other cases, the grout and pipe conductivity and BHE depth were varied according to the information provided in Table 2.

| Stockholm 2 × 107 m | |
| --- | --- |
| Ground | |
| Thermal conductivity | 3.5 W/(m·K) |
| Heat capacity | 2.16 MJ/(m$^3$·K) |
| Surface temperature | 7.6 °C |
| Geothermal heat flux | 0.05 W/m$^2$ |
| Borehole | |
| Configuration | 1 × 2 line |
| Depth | 107 m |
| Borehole Spacing | 10 |
| Borehole Installation | Single U |
| Borehole Diameter | 120 mm |
| U-pipe diameter | 32 mm |
| U-pipe thickness | 3 mm |
| U-pipe thermal conductivity | 0.42 W/(m·K) |
| U-pipe shank spacing | 60 mm |
| Filling thermal conductivity | 2 W/(m·K) |
| Contact resistance pipe/filling | 0 m·K/W |
| Thermal Resistances | |
| Number of multipoles | 10 |
| Heat Carrier Fluid | |
| Thermal conductivity | 0.48 W/(m·K) |
| Specific heat capacity | 3795 J/(Kg·K) |
| Density | 1052 Kg/m$^3$ |
| Viscosity | 0.0052 Kg/(m·s) |
| Freezing point | −14 °C |
| Flow rate per borehole | 2 L/s |

### 3.3. The Modelled Building

The typical European residential house as defined by the EU ENTRANZE project was considered in this study [44]. The modelling of the house was performed in DesignBuilder using the building geometry and characteristics from the same project. The overview of the DesignBuilder model and building plans for first and ground floors are presented in Figure 4, Figure 5, and Figure 6, respectively.
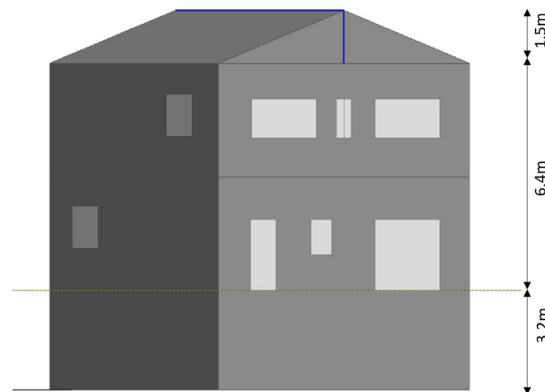
**Figure 4.** Model overview of a typical house in Europe, as defined by the European EN-TRANZE project [44].
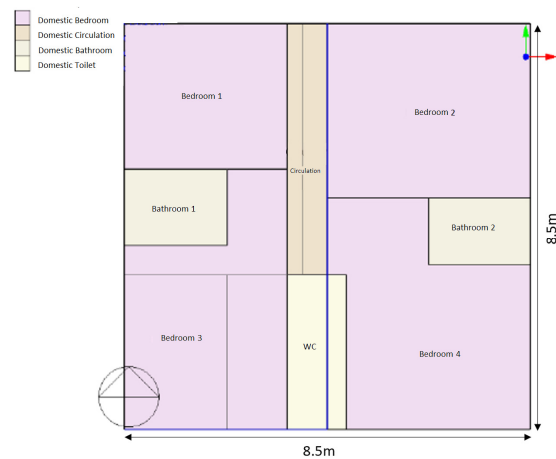


**Figure 5.** First floor plan view.
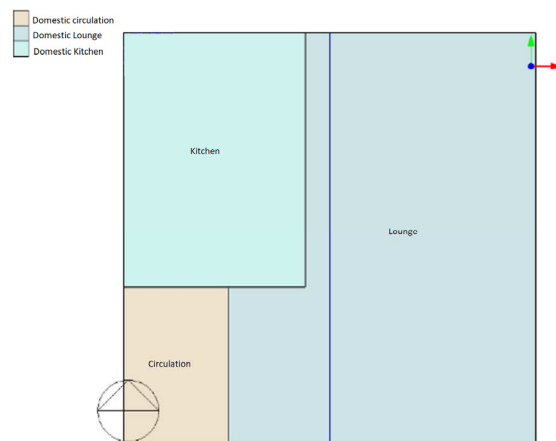


**Figure 6.** Ground floor plan view.

The model was validated using data published in the ENTRANZE project's results, for a warm climate (Madrid), where the cumulative annual heating and cooling demand was 151.6 kWh/m$^2$. The modelled heating and cooling demand were 40 kWh/m$^2$ and 108.5 kWh/m$^2$, respectively. This corresponds to a difference of 3 kWh/m$^2$ (or 2% error) in the cumulative space conditioning energy demand. The modelled cooling demand for Valencia based on calibration for Madrid is presented in Figure 7. For Stockholm, a similar calibration was carried out and is shown in Figure 8. The figures clearly depict the difference in the two climates considered—Stockholm has negligible cooling, while for

Valencia, it is cooling that is the greater space conditioning demand over the year. The total space conditioning energy demand for Valencia and Stockholm accrues to 101.8 kWh/m$^2$ and 123.3 kWh/m$^2$, respectively. The hourly load profiles are then used in EED to size the BHE to fulfil this demand as described in the following section.
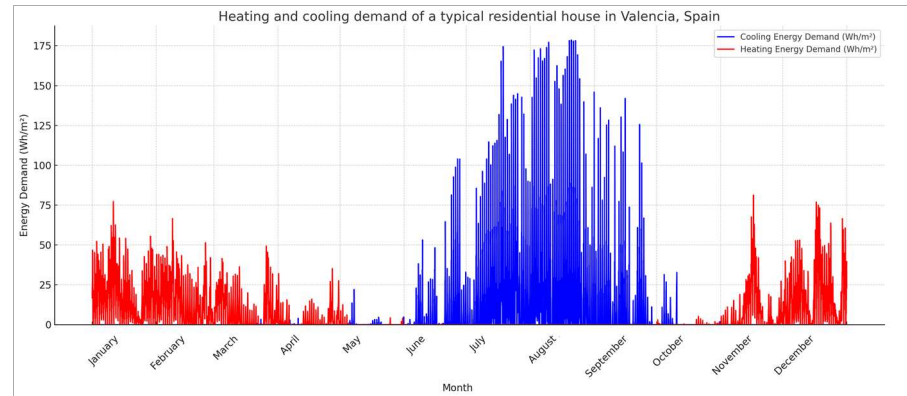


**Figure 7.** Simulated demand profile for Valencia based on a calibrated model. Cooling demand: 53.5 kWh/m$^2$/year, heating demand: 48.3 kWh/m$^2$/year.
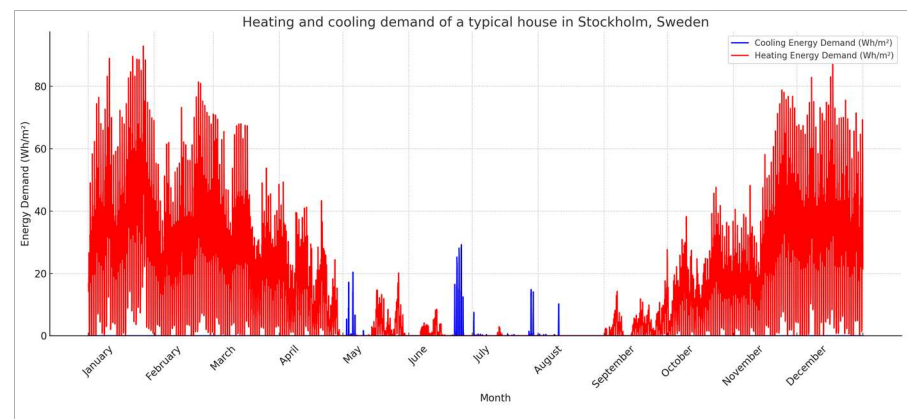


**Figure 8.** Simulated demand profile for Stockholm based on a calibrated model. Cooling demand: 0.8 kWh/m$^2$, heating demand: 122.5 kWh/m$^2$.

Exergetic Indicators for Performance Analysis

The following exergetic performance metric were used to assess thermodynamic performance:

BHE exergy extracted: Heat can flow into or out of the BHE depending on whether heating or cooling is required in the building. As exergy is the variation from a thermodynamic reference, which in this case is the local weather, heat flowing into the BHE during winter and heat flowing out the BHE during summer can both be counted as exergy extracted by the BHE. The return fluid temperature in the borehole is considered the BHE boundary temperature, while the outdoor air temperature is the reference temperature $T_0$. Using these assumptions and definitions, the exergy extracted by the BHE is calculated using Equation (2), where "Q" is the heat transfer to or from the BHE. The exergy efficiency of a system in general is given by:

$$\eta_{Ex} = \frac{Useful\ output\ exergy}{Supplied\ input\ exergy} \qquad (4)$$

For the GSHP case, the supplied input exergy is electricity, which is pure work (quality factor of one). The useful output is the delivered heating and cooling, which corresponds

to the exergy demand of the building. Based on a setpoint temperature of 18 °C, the exergy efficiency is calculated as follows:

$$\eta_{Ex} = \frac{Exergy\ demadn}{HP\ Electricity\ input} = \frac{Energy\ demand\ \left(1 - \frac{T_0}{291.15}\right)}{HP\ Electricity\ input} \tag{5}$$

## 4. Results and Discussion

Utilizing the methodology presented earlier, the results were generated for the two locations. A summary of the results for the exergy analysis are presented in Table 2. The exergy efficiency of the GSHPs ranged from 11.6–25.9% across the different scenarios, which is similar to studies reported in the literature review (Section 3). Moreover, it can be observed that the location with cooling dominated climate had a higher exergy efficiency, which is also in agreement with previously reported work [34].

**Table 2.** Results of the exergy analysis based on annual hourly simulation data.

| | Energy Demand | Exergy Demand | BHE Exergy Extracted | BHE Exergy Extracted Improvement | BHE Exergy Proportion | Electricity Demand | GSHP Exergy Efficiency |
|---|---|---|---|---|---|---|---|
| | kWh | kWh | kWh | % | % of total | kWh | % |
| | | | | Stockholm 2 × 107 m | | | |
| Baseline | 17,833 | 1166 | 235 | 0 | 20.15 | 4596 | 25.37 |
| Semi-GEOCOND | 17,833 | 1166 | 247 | 5.11 | 21.18 | 4554 | 25.6 |
| GOCOND | 17,833 | 1166 | 265 | 12.77 | 22.73 | 4497 | 25.93 |
| | | | | Stockholm 1 × 190 m | | | |
| Baseline | 17,833 | 1166 | 333 | 0 | 28.56 | 4786 | 24.36 |
| Semi-GEOCOND | 17,833 | 1166 | 349 | 4.8 | 29.93 | 4763 | 24.48 |
| GOCOND | 17,833 | 1166 | 376 | 12.91 | 32.25 | 4727 | 24.67 |
| | | | | Valencia 2 × 80 m | | | |
| Baseline | 14,366 | 378.22 | 229 | 0 | 60.55 | 3655 | 10.35 |
| Semi-GEOCOND | 14,382 | 384.9 | 219 | −4.37 | 56.9 | 3591 | 10.72 |
| GOCOND | 14,398 | 407.7 | 209.8 | −8.38 | 51.46 | 3513 | 11.61 |

The observed exergy efficiency is notably low, which stems from the substantial exergy destruction during the conversion from electricity to low-grade heat. Taking the Stockholm baseline scenario as an illustration, an annual energy demand of 17,833 kWh translates to merely 1166 kWh of exergy, which is met using 4596 kWh of electricity. This conversion process results in most of the electrical exergy, specifically 3430 kWh annually or 75%, being lost to what is termed as exergy destruction due to energy quality degradation. In the context of Valencia, this exergy destruction is even more pronounced, accounting for 88.6% of the provided electricity.

This heightened loss in Valencia can be attributed to the disparity between the indoor setpoint (established at 18 °C in this analysis) and the outdoor dry bulb temperature. As portrayed in Figure 9, the outdoor temperature in Stockholm exhibits a more pronounced deviation from the indoor setpoint, averaging 12 °C in contrast to Valencia's modest 5.6 °C. Stockholm's larger temperature differential suggests a heightened energy quality demand, fostering a more harmonious match between energy supply and demand. Furthermore, Figure 9 underscores the pivotal role of indoor temperature setpoint selection. Although 18 °C might be a conventional choice, various strategies exist that advocate for a dynamic indoor setpoint [45–48], which would undeniably have a profound impact on the exergy destruction within the building.
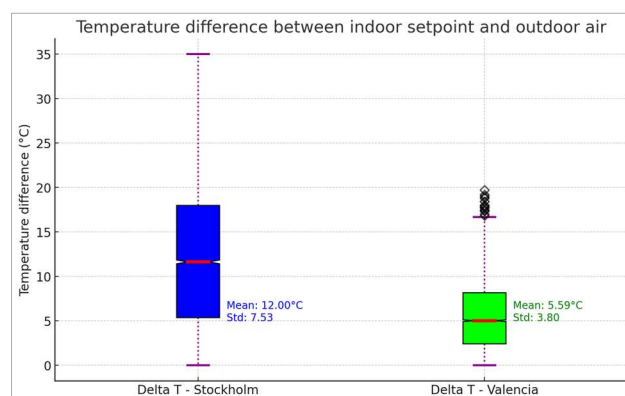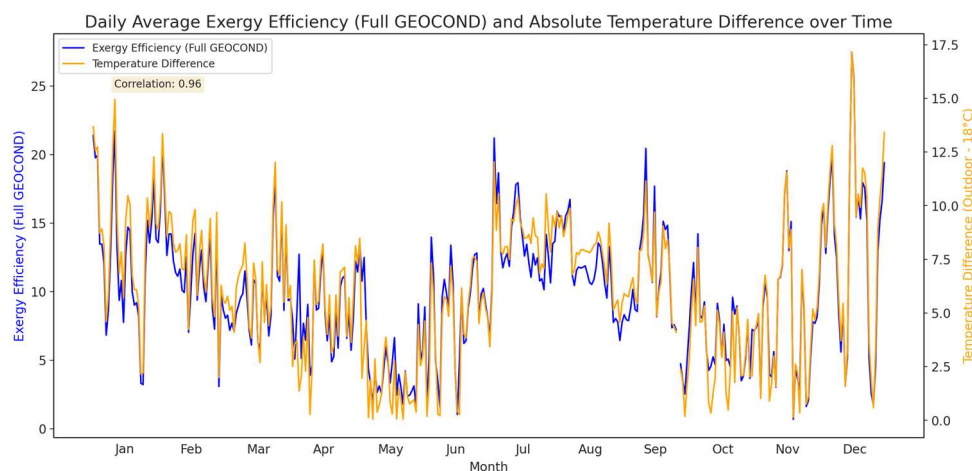
**Figure 9.** Indoor setpoint vs. outdoor temperature delta. Greater difference in Stockholm (12 °C vs. 5.59 °C in Valencia) implies higher energy quality demand for building space conditioning.

The efficacy of the borehole heat exchanger (BHE) from a thermodynamic standpoint can be gauged by the exergy it extracts. As Table 2 illustrates, the proportion of exergy the BHE extracts relative to the total fluctuates between 20.2% and 60.6% across diverse scenarios. In Stockholm's context, the introduction of GEOCOND materials amplifies BHE extraction by 30 kWh/year and 43 kWh/year for depths of 107 m and 190 m, respectively. This signifies a 13% enhancement in BHE extraction and a reduction of 99 kWh electricity demand per year compared to the conventional baseline for both depth variants. Notably, the deeper BHE variant (190 m) boasts a markedly superior exergy extraction capacity, constituting 32% of the total supply compared to the 23% seen in the GEOCOND scenario. Such efficiency is achieved in tandem with a 24 m reduction in BHE length, potentially translating to cost savings during the installation phase. As for Valencia, a minor decrement in the percentage of total energy input extracted by the BHE ensues, but this is offset by a 0.84% enhancement in exergy efficiency. This subtle advancement likely stems from the minimal temperature discrepancy between the outdoors and the indoor setpoint, as depicted in Figure 9.

Figure 10 further sheds lights on the relationship between exergy efficiency and the variance between outdoor temperature and the indoor setpoint. Specifically in Valencia, as the outdoor dry bulb temperature converges with the indoor setpoint, exergy efficiency tends to zero, stemming from the decreasing energy demand quality. This relationship is further corroborated by an $R^2$ value of 0.96, showing the strong correlation between the two metrics. Observing the temperature delta showcased in Figure 10, it is evident that space conditioning is inherently a low-grade energy demand. This accentuates the significance of indoor setpoint selection as a crucial determinant influencing the exergetic performance of building space conditioning systems.

The findings of the present study offer an understanding of how high-thermal-conductivity pipe and grout materials may impact the exergy efficiency in building space conditioning systems. The thermal conductivity of grout and pipe has indeed been identified in several studies to be an important factor in BHE performance. For example, Kim and Oh [49] investigated the effect sand and water proportion in cementitious grouts, with a max thermal conductivity of 1.87 W/mK achieved. In an effort to identify the optimum parameters for high performing BHEs, Tang and Nowamooz [13] conducted a numerical simulation study and analysed 15 parameters that can affect BHE performance but also the overall COP of the heat pump. Their grout and pipe thermal conductivity parameter space were 0.8–3.2 W/mK and 0.25–16 W/mK respectively. Their results showed that pipe thermal conductivity beyond 2 W/mK makes little difference, but increased thermal conductivity in the grout does result in increased COP, even at values in excess of 3 W/mK. In addition to these factors, they found that meteorological conditions, pipe configuration, and the heat load level could influence the BHE's annual performance significantly. In line with this, Badenes et al. [5] conducted a comprehensive parameter study aiming to

identify the best material specifications for both pipes and grouts, identifying various target material properties. According to their numerical study, the required thermal conductivity of the grout and pipe should be 2–4 W/mK and approximately 1 W/mK, respectively. In an effort to achieve such values, Liu et al. [50] investigated the potential of quartz sand–bentonite–carbon fibre mixtures for grout materials and reported a maximum of 1.98 W/mK. In a similar effort, Dong et al. [4] used the addition of silica in cementitious grouts to achieve 2.1 W/mK. However, higher grout thermal conductivity values have recently been reported in a study by Mascarin et al. [51], in which expanded graphite is highlighted as a material which generally enhances thermal properties, with values of up to 3 W/mK achievable.



**Figure 10.** Effect of outdoor temperature and its variation from setpoint on exergy efficiency for Valencia. All data are 24 h averaged.

The grout and pipe thermal conductivity values thus achieved in the GEOCOND project (1 W/mK and 3 W/mK for the pipe and grout, respectively) are certainly at the higher end of the spectrum, where the impact of such high thermal conductivity values has been assessed at the BHE and heat pump, using energy and exergy analysis. For instance, in Stockholm, using materials with higher thermal conductivity could reduce the required length of the system by 13% and increase its efficiency by the same amount, which agrees with the literature [5,50,51]. However, in Valencia, despite the high conductivity, the efficiency remained relatively low, between 10–12%. This difference between the two locations shows that local weather and building temperature settings can greatly influence system performance [13,45–48] and therefore should be considered carefully when designing BHEs for GSHPs.

## 5. Conclusions and Recommendations

This study presents an analysis of the potential thermodynamic enhancements achievable through the utilization of high-conductivity grout and pipe materials, as introduced in the GEOCOND project, with the aid of computer simulations. The salient insights derived from our analysis include:

- **Enhanced BHE Exergy Extraction:** The adoption of pipe and grout materials boasting thermal conductivities of 1 W/mK and 3 W/mK, respectively, can usher in notable improvements in the exergy extraction capabilities of the borehole heat exchanger (BHE). This assertion is substantiated by the observed 13% enhancement for the Stockholm scenario. This uptick subsequently curtails the GSHP's electricity requisites by approximately 99 kWh/year, a factor with direct economic ramifications spanning the entire use phase of the life cycle.
- **Regional Variations in Exergetic Performance:** For Valencia, the exergetic gains were found to be rather marginal. Additionally, the average exergy efficiency in Valencia trailed at roughly 11%, as opposed to Stockholm's more robust 25%. A pivotal

takeaway from our analysis underscores the dependency of exergy efficiency—and the scope for thermodynamic augmentation via high-conductivity materials—on external factors like the outdoor dry bulb temperature and its deviation from the indoor setpoint.

- **Advantages of Increased BHE Depth:** A deeper BHE (1 × 190 m in contrast to 2 × 107 m) results in more potent exergy extraction. This depth increment not only results in exergy efficiency that rivals the shallower BHE but also achieves this with a 24 m reduction in total BHE length. It is imperative to note, however, that this study didn't encompass potential variations in electricity demands due to pumping, which could be influenced by the increased depth.

- **Exergy Loss Due to Energy Quality Degradation:** Within the GSHP energy paradigm, the most pronounced exergy drain stems from the inevitable quality degradation as electricity morphs into low-grade heat. This accounted for a significant 77% loss for Stockholm and an even steeper 89% for Valencia. These figures accentuate the importance of energy quality alignment between supply and demand mechanisms.

These results provide useful information on the GSHP's use phase part of the life cycle, which can be utilized to derive costs over its operational lifetime and integrated into a full life cycle analysis. However, these results are limited to only two locations, and it would be beneficial to conduct an exploratory study to include various locations and climates in Europe or globally. In terms of low carbon solutions, it would be useful to investigate the amount of exergy (electricity) that solar PV (or a variant of it) could offset from the electricity requirements of a GSHP system in the typical house with respect to different locations and climates. As the location has a major impact on (i) the achievable exergetic improvements using high conductivity materials, and (ii) the amount of electricity generated by solar PV, this is recommended as future work. The results of such a study would indicate where the high conductivity materials such as those developed in the GEOCOND project would be most fruitful in terms of delivering cost effective environmentally friendly space conditioning in buildings.

**Conflicts of Interest:** The authors declare no conflict of interest.

## References

1. Thomaßen, G.; Kavvadias, K.; Jiménez Navarro, J.P. The decarbonisation of the EU heating sector through electrification: A parametric analysis. *Energy Policy* **2021**, *148*, 111929. [CrossRef]
2. Huang, B.; Mauerhofer, V. Life cycle sustainability assessment of ground source heat pump in Shanghai, China. *J. Clean. Prod.* **2016**, *119*, 207–214. [CrossRef]
3. Bonamente, E.; Aquino, A. Environmental performance of innovative ground-source heat pumps with PCM energy storage. *Energies* **2019**, *13*, 117. [CrossRef]
4. Dong, S.; Liu, G.; Zhan, T.; Yao, Y.; Ni, L. Performance Study of Cement-Based Grouts Based on Testing and Thermal Conductivity Modeling for Ground-Source Heat Pumps. *Energy Build.* **2022**, *272*, 112351. [CrossRef]

5.  Badenes, B.; Sanner, B.; Mateo Pla, M.Á.; Cuevas, J.M.; Bartoli, F.; Ciardelli, F.; González, R.M.; Ghafar, A.N.; Fontana, P.; Lemus Zuñiga, L.; et al. Development of advanced materials guided by numerical simulations to improve performance and cost-efficiency of borehole heat exchangers (BHEs). *Energy* **2020**, *201*, 117628. [CrossRef]
6.  Zhou, Y.; Zhang, Y.; Xu, Y. Influence of Grout Thermal Properties on Heat-Transfer Performance of Ground Source Heat Exchangers. *Sci. Technol. Built Environ.* **2018**, *24*, 461–469. [CrossRef]
7.  Frąc, M.; Szudek, W.; Szołdra, P.; Pichór, W. Grouts with Highly Thermally Conductive Binder for Low-Temperature Geothermal Applications. *Constr. Build. Mater.* **2021**, *295*, 123680. [CrossRef]
8.  Dong, S.; Liu, G.; Zhan, T.; Yao, Y.; Ni, L. A Thermal Conductivity Prediction Model of Cement-Based Grouts for Ground Source Heat Pump. *Int. Commun. Heat Mass Transf.* **2022**, *135*, 106079. [CrossRef]
9.  Huang, Y.; Zhang, Y.; Xie, Y.; Zhang, Y.; Gao, X. Thermal Performance Analysis on the Composition Attributes of Deep Coaxial Borehole Heat Exchanger for Building Heating. *Energy Build.* **2020**, *221*, 110019. [CrossRef]
10. Mahon, H.; O'Connor, D.; Friedrich, D.; Hughes, B. A Review of Thermal Energy Storage Technologies for Seasonal Loops. *Energy* **2022**, *239*, 122207. [CrossRef]
11. Deng, Y.; Feng, Z.; Fang, J.; Cao, S.J. Impact of Ventilation Rates on Indoor Thermal Comfort and Energy Efficiency of Ground-Source Heat Pump System. *Sustain. Cities Soc.* **2018**, *37*, 154–163. [CrossRef]
12. Habibi, M.; Hakkaki-Fard, A. Long-Term Energy and Exergy Analysis of Heat Pumps with Different Types of Ground and Air Heat Exchangers. *Int. J. Refrig.* **2019**, *100*, 414–433. [CrossRef]
13. Tang, F.; Nowamooz, H. Factors influencing the performance of shallow Borehole Heat Exchanger. *Energy Convers. Manag.* **2019**, *181*, 571–583. [CrossRef]
14. Khattak, S.H.; Brown, N.; Greenough, R. Suitability of exergy analysis for industrial energy efficiency, manufacturing and energy management. In Proceedings of the ECEEE 2012 Summer Study on Energy Efficiency in Industry, Arnhem, The Netherlands, 11–14 September 2012; pp. 237–245.
15. Yantovski, E. What Is Exergy? *Ecos* **2004**, *2004*, 7–9.
16. Kizilkan, O.; Dincer, I. Borehole thermal energy storage system for heating applications: Thermodynamic performance assessment. *Energy Convers. Manag.* **2015**, *90*, 53–61. [CrossRef]
17. Lucia, U.; Simonetti, M.; Chiesa, G.; Grisolia, G. Ground-source pump system for heating and cooling: Review and thermodynamic approach. *Renew. Sustain. Energy Rev.* **2017**, *70*, 867–874. [CrossRef]
18. Kerdan, I.G.; Raslan, R.; Ruyssevelt, P. Dynamic exergy simulation coupled with thermoeconomic analysis to support retrofit decisions in non-domestic buildings. *Future* **2014**, *52*, 1.
19. Khattak, S.H.; Greenough, R.; Korolija, I.; Brown, N. An exergy based method to resource accounting for factories. *J. Clean. Prod.* **2015**, *121*, 99–108. [CrossRef]
20. Khattak, S.H.; Oates, M.; Greenough, R. Towards Improved Energy and Resource Management in Manufacturing. *Energies* **2018**, *11*, 1006. [CrossRef]
21. Hepbasli, A.; Kalinci, Y. A review of heat pump water heating systems. Renew. Sustain. *Energy Rev.* **2009**, *13*, 1211–1229. [CrossRef]
22. Tsatsaronis, G. Definitions and nomenclature in exergy analysis and exergoeconomics. *Energy* **2007**, *32*, 249–253. [CrossRef]
23. Bakshi, B.R.; Gutowski, T.G.P.; Sekulić, D.P. *Thermodynamics and the Destruction of Resources*; Cambridge University Press: New York, NY, USA, 2011; ISBN 0521884551.
24. Gundersen, T. *An Introduction to the Concept of Exergy and Energy Quality*; Department of Energy and Process Engineering Norwegian University of Science and Technology: Trondheim, Norway, 2010; Version 4.
25. Schmidt, D.; Ala-Juusela, M. Low Exergy Systems for Heating and Cooling of Buildings. Available online: https://alexandria.tue.nl/openaccess/635611/p0595final.pdf (accessed on 27 August 2023).
26. Shukuya, M.; Hammache, A. Introduction to the concept of exergy. In *Low Exergy Systems for Heating and Cooling of Buildings*; IEA Annex Finl.; 2002; pp. 41–44, ISBN 951-38-6075-2. Available online: http://www.inf.vtt.fi/pdf/ (accessed on 30 April 2023).
27. Hepbasli, A. Low exergy (LowEx) heating and cooling systems for sustainable buildings and societies. *Renew. Sustain. Energy Rev.* **2012**, *16*, 73–104. [CrossRef]
28. Helena, T.; Schmidt, D. ECBCS Annex 49—Low Exergy Systems for High-Performance Buildings and Communities. In *Exergy Assessment Guidebook for the Built Environment*; Summary Report; Fraunhofer IBP: Kassel, Germany, 2011; ISBN 9783839602393.
29. Lohani, S.P.; Schmidt, D. Comparison of energy and exergy analysis of fossil plant, ground and air source heat pump building heating system. *Renew. Energy* **2010**, *35*, 1275–1282. [CrossRef]
30. Hu, P.; Hu, Q.; Lin, Y.; Yang, W.; Xing, L. Energy and exergy analysis of a ground source heat pump system for a public building in Wuhan, China under different control strategies. *Energy Build.* **2017**, *152*, 301–312. [CrossRef]
31. Verda, V.; Cosentino, S.; Russo, S.L.; Sciacovelli, A. Second law analysis of horizontal geothermal heat pump systems. *Energy Build.* **2016**, *124*, 236–240. [CrossRef]
32. Erbay, Z.; Hepbasli, A. Application of conventional and advanced exergy analyses to evaluate the performance of a ground-source heat pump (GSHP) dryer used in food drying. *Energy Convers. Manag.* **2014**, *78*, 499–507. [CrossRef]
33. Ally, M.R.; Munk, J.D.; Baxter, V.D.; Gehl, A.C. Exergy analysis of a two-stage ground source heat pump with a vertical bore for residential space conditioning under simulated occupancy. *Appl. Energy* **2015**, *155*, 502–514. [CrossRef]

34. Menberg, K.; Heo, Y.; Choi, W.; Ooka, R.; Choudhary, R.; Shukuya, M. Exergy analysis of a hybrid ground-source heat pump system. *Appl. Energy* **2017**, *204*, 31–46. [CrossRef]

35. Kayaci, N. Energy and exergy analysis and thermo-economic optimization of the ground source heat pump integrated with radiant wall panel and fan-coil unit with floor heating or radiator. *Renew. Energy* **2020**, *160*, 333–349. [CrossRef]

36. EnergyPlus Weather Data. Available online: https://energyplus.net/weather-region/europe_wmo_region_6 (accessed on 7 September 2020).

37. Nordman, R.; Zottl, A.; Miara, M.; Huber, H. System boundaries for SPF-calculation. In Proceedings of the 10th IEA Heat Pump Conference, Tokyo, Japan, 16–19 May 2011; pp. 16–19.

38. Designbuilder Software Limited Design Builder. Available online: http://www.designbuilder.co.uk/ (accessed on 10 January 2023).

39. Blocon, A.B. Earth Energy Designer 4.20 (EED 4.20). Available online: https://buildingphysics.com/eed-2/ (accessed on 27 August 2023).

40. Bohne, D.; Wohlfahrt, M.; Harhausen, G.; Sanner, B.; Mands, E.; Sauer, M.; Grundmann, E. Geothermal Monitoring of eight non-residential buildings with heat and cold production–experiences, results and optimization. In Proceedings of the 12th International Conference on Energy Storage, Lleida, Spain, 16–18 May 2012.

41. Sanner, B.; Bockelmann, F.; Kühl, L.; Mands, E. System optimisation of ground-coupled heat and-cold supply of office buildings. In Proceedings of the European Geothermal Congress, Strasbourg, France, 19–24 September 2016.

42. Ochsner Heat Pumps GMSW 28 HK Monovalent Heating System with Brine as a Heat Source. 2021. Available online: https://www.ochsnerengineering.com/gmsw-28-hk/ (accessed on 20 July 2021).

43. Curtis, R.; Lund, J.; Sanner, B.; Rybach, L.; Hellström, G. Ground source heat pumps–geothermal energy for anyone, anywhere: Current worldwide activity. In Proceedings of the World Geothermal Congress, Antalya, Turkey, 24–29 April 2005; pp. 24–29.

44. Zangheri, P.; Armani, R.; Pietrobon, M.; Pagliano, L.; Fernandez Boneta, M.; Müller, A. *Heating and Cooling Energy Demand and Loads for Building Types in Different Countries of the EU*; The ENTRANZE Project; Intelligent Energy Europe Programme of the European Union; 2014; p. 86. Available online: https://www.entranze.eu/files/downloads/D2_3/Heating_and_cooling_energy_demand_and_loads_for_building_types_in_different_countries_of_the_EU.pdf (accessed on 27 August 2023).

45. Khattak, S.H.; Natarajan, S.; Chung, W.J. Out with the power outages: Peak load reduction in the developing world. In Proceedings of the Windsor 2020 Resilient Comfort, Windsor, UK, 16–19 April 2020; pp. 904–922.

46. Hoyt, T.; Arens, E.; Zhang, H. Extending air temperature setpoints: Simulated energy savings and design considerations for new and retrofit buildings. *Build. Environ.* **2015**, *88*, 89–96. [CrossRef]

47. Traylor, C.; Zhao, W.; Tao, Y.X. Utilizing modulating-temperature setpoints to save energy and maintain alliesthesia-based comfort. *Build. Res. Inf.* **2019**, *47*, 190–201. [CrossRef]

48. Chung, W.J.; Park, S.H.; Yeo, M.S.; Kim, K.W. Control of thermally activated building system considering zone load characteristics. *Sustainability* **2017**, *9*, 586. [CrossRef]

49. Kim, D.; Oh, S. Relationship between the thermal properties and degree of saturation of cementitious grouts used in vertical borehole heat exchangers. *Energy Build.* **2019**, *201*, 1–9. [CrossRef]

50. Liu, L.; Cai, G.; Liu, X.; Liu, S.; Puppala, A.J. Evaluation of thermal-mechanical properties of quartz sand–bentonite–carbon fiber mixtures as the borehole backfilling material in ground source heat pump. *Energy Build.* **2019**, *202*, 109407. [CrossRef]

51. Mascarin, L.; Garbin, E.; Di Sipio, E.; Dalla Santa, G.; Bertermann, D.; Artioli, G.; Bernardi, A.; Galgaro, A. Selection of backfill grout for shallow geothermal systems: Materials investigation and thermo-physical analysis. *Constr. Build. Mater.* **2022**, *318*, 125832. [CrossRef]